Quantifying the seasonal "breathing" of the Antarctic ice sheet

S. R. M. Ligtenberg,[1] M. Horwath,[2] M. R. van den Broeke,[1] and B. Legrésy[3]

Received 21 August 2012; revised 1 November 2012; accepted 4 November 2012; published 13 December 2012.

[1] One way to estimate the mass balance of an ice sheet is to convert satellite observed surface elevation changes into mass changes. In order to do so, elevation and mass changes due to firn processes must be taken into account. Here, we use a firn densification model to simulate seasonal variations in depth and mass of the Antarctic firn layer, and assess their influence on surface elevation. Forced by the seasonal cycle in temperature and accumulation, a clear seasonal cycle in average firn depth of the Antarctic ice sheet (AIS) is found with an amplitude of 0.026 m, representing a volume oscillation of 340 km^3. The phase of this oscillation is rather constant across the AIS: the ice sheet volume increases in austral autumn, winter and spring and quickly decreases in austral summer. Seasonal accumulation differences are the major driver of this annual 'breathing', with temperature fluctuations playing a secondary role. The modeled seasonal elevation signal explains ~31% of the seasonal elevation signal derived from ENVISAT radar altimetry, with both signals having similar phase. **Citation:** Ligtenberg, S. R. M., M. Horwath, M. R. van den Broeke, and B. Legrésy (2012), Quantifying the seasonal "breathing" of the Antarctic ice sheet, *Geophys. Res. Lett.*, *39*, L23501, doi:10.1029/2012GL053628.

1. Introduction

[2] The Antarctic ice sheet (AIS) is the largest reservoir of frozen water on Earth, containing the equivalent ice volume of 57 m global sea level rise [*Lythe et al.*, 2001]. With an annual mass turnover of ~2500 Gt [*Lenaerts et al.*, 2012], even a relatively small change in the mass balance of the AIS has a significant effect on global sea level [*Intergovernmental Panel on Climate Change*, 2007; *Van den Broeke et al.*, 2011]. Estimating the mass balance of the AIS is difficult, because of its size, remoteness and the fact that it has only been studied intensively during the last half century. Currently, three methods are used for estimating the mass balance of the AIS: i) the mass budget method [*Rignot et al.*, 2011], ii) the gravimetry method [*Velicogna*, 2009] and iii) the volumetric method [*Davis et al.*, 2005]. In the latter method, remotely sensed surface elevation (volume) changes are converted into mass changes. This conversion requires a correction for depth and mass changes of the firn layer, the mantle of compressed snow that covers the AIS.

[3] Neglecting basal melt, the vertical movement of the ice sheet surface (dH/dt) is forced by snow accumulation (v_{acc}), sublimation (included in v_{acc}), snowmelt (v_{me}), firn compaction (v_{fc}), ice flow beneath the firn layer (v_{ice}), and buoyancy effects on floating ice shelves (v_{by}) [*Ligtenberg et al.*, 2011]:

$$\frac{dH}{dt} = v_{acc} + v_{me} + v_{fc} + v_{ice} + v_{by} \quad (1)$$

Following the seasonal cycle in temperature and accumulation, which affects v_{acc}, v_{me} and v_{fc}, the firn layer covering the ice sheets of Antarctica and Greenland 'breathes', i.e., it expands in winter and contracts in summer. Although this phenomenon is often mentioned in literature [e.g., *Thomas et al.*, 2008; *Lee et al.*, 2012], it has not yet been robustly quantified. For the Greenland firn layer, *Braithwaite et al.* [1994] suggested seasonal oscillations in surface elevation of 0.1–0.2 m, while *Zwally and Li* [2002] observed (0.25 m) and modeled (0.18 m) similar seasonal variations at Summit, Greenland. The only Antarctic observation suggests seasonal variations up to 0.6 m based on radar satellite altimetry [*Yi et al.*, 1997]. All studies report surface elevation minima in mid- or late summer and maxima in late winter. These regular oscillations in surface elevation can be important when deriving surface elevation trends from satellite altimetry, especially in the case of short time series with sparse sub-annual sampling [*Gunter et al.*, 2009]. In this study, we combine output of a regional atmospheric climate model at relatively high horizontal resolution (~27 km) with a firn densification model to quantify this effect for the AIS. We compare apparent volume changes inferred from ENVISAT satellite radar altimetry (RA) to modeled volume changes.

2. Methods

[4] We use a 1D, time-dependent firn densification model (FDM) that calculates temperature, density and liquid water content in a vertical firn column with a typical layer thickness of 5 cm [*Ligtenberg et al.*, 2011]. At the surface, the FDM is forced by 6 hour cumulated surface mass balance components (snowfall, rain, sublimation and snowmelt) and 6 hour average surface temperature (T_s) and 10 m windspeed from a regional atmospheric climate model (RACMO2) at ~27 km horizontal resolution [*Lenaerts et al.*, 2012]. To obtain initial vertical firn profiles a spin-up procedure is used: sufficient iterations of the 1979–2011 climate are used to build up a complete firn layer, before the final run is performed [*Ligtenberg et al.*, 2011]. This approach assumes a stable climate for the past 100–200 years, i.e., no significant long-term (centennial) trends in temperature or accumulation. The final FDM run covers the 1979–2011 period with a time step of 15 minutes and output is stored every

[1]Institute for Marine and Atmospheric Research Utrecht, Utrecht University, Utrecht, Netherlands.
[2]Institut für Astronomische und Physikalische Geodäsie, Technische Universität München, Munich, Germany.
[3]Laboratoire d'Etudes en Géophysique et Océanographie Spatiales, Toulouse, France.

Corresponding author: S. R. M. Ligtenberg, Institute for Marine and Atmospheric Research Utrecht, PO Box 80.000, NL-3508 TA Utrecht, Netherlands. (s.r.m.ligtenberg@uu.nl)

0094-8276/12/2012GL053628

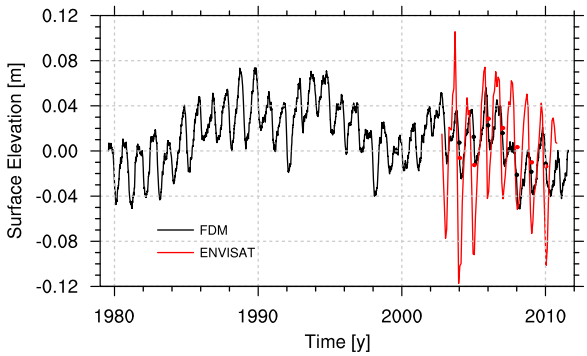

Figure 1. Ice sheet averaged surface elevation time series as simulated by the firn densification model (FDM, black) and as observed by the ENVISAT radar altimeter (ENVISAT, red). Dots indicate one-year surface elevation averages for the FDM (black) and ENVISAT (red). A 0.01 m surface elevation change is equal to a 131 km^3 (FDM) or 98 km^3 (ENVISAT) firn volume anomaly, because of the different areas of coverage (see Figures 4a–4c).

2 days. In this paper we present i) changes in monthly surface elevation, e.g., a dH/dt value for January represents the change in surface elevation between the 31st of December and the 31st of January and ii) the amplitude and phase of a sine function fitted to the average seasonal surface elevation oscillations.

[5] We compare FDM results to ENVISAT radar altimetry data for the period October 2002 through October 2010, derived from the along-track repeat satellite RA approach [*Legrésy et al.*, 2006]. This approach analyses time series of altimetric observations at every along-track position along the 35-day repeat orbit. The effect of non-exact repeat positions in conjunction with local topography is corrected empirically. Time variable relative contributions of surface and volume echos are corrected using the echo shape corrections [*Legrésy et al.*, 2006]. *Horwath et al.* [2012] showed that having time series of RA corrected from the echo shape time variations makes them qualitatively consistent to GRACE observations at interannual and longer terms. The polar gap (south of 81.5°S), steep terrain areas and floating ice shelves are excluded from the RA dataset.

3. Results

[6] Figure 1 shows the modeled surface elevation evolution averaged over the AIS, including its floating ice shelves, for the period 1979–2011. The seasonal cycle explains 30% of the total temporal variability, i.e., significant interannual variability exists. For instance, the surface of the AIS rose on average by ~7 cm between 1979 and 1989, and fell by ~5 cm in each of the periods 1994–2000 and 2006–2009. These interannual variations are mainly associated with snowfall variability, as was also shown by *Davis et al.* [2005], *Helsen et al.* [2008] and *Horwath et al.* [2012]. Part of these variations is also explained by the steady state assumption that is made in the FDM (see Section 2 and *Ligtenberg et al.* [2011]), forcing the surface elevation to start and end at zero. Long-term accumulation variability could add up to 8% uncertainty in long-term surface elevation trends, while long-term snowmelt variability can increase the uncertainty by up to 30% [*Pritchard et al.*, 2012].

[7] In Figure 2, the average seasonal cycle of the surface elevation and its separate components from Equation 1 are shown. By definition, v_{ice} is constant throughout the year, and its magnitude equals the average annual accumulation rate divided by the ice density. The buoyancy effect (v_{by}) of the floating parts of the ice sheet, the coastal ice shelves, is small when averaged over the full AIS, and only locally important [*Pritchard et al.*, 2012]. Melting of snow (v_{me}) is only significant in summer and in the coastal regions of the AIS, where it forces a downward surface velocity mainly in December and January. Sublimation, which is incorporated in v_{acc}, has two components: surface sublimation, which peaks in summer, and drifting snow sublimation, which peaks in winter [*Lenaerts and Van den Broeke*, 2012]. However, the seasonal cycle in v_{acc} is dominated by the winter maximum in snowfall [*Lenaerts et al.*, 2012]. Firn compaction (v_{fc}) shows a relatively weak seasonal cycle, driven by enhanced compaction in summer and early winter, when the summer heat wave penetrates the firn pack. All processes combined result in a strongly negative dH/dt (v_{tot}) in December and January, when surface temperature, densification rate, snowmelt and surface sublimation peak. In combination with low accumulation this leads to rapid lowering of the surface. In autumn, winter and spring, the surface steadily rises under influence of enhanced winter snow accumulation and reduced densification rates, snowmelt and surface sublimation. In contrast to summer, there is no clear peak in winter surface rise.

[8] Figure 3 shows that the seasonal cycle in surface elevation is spatially consistent across the AIS. In January, dH/dt is negative over most of the AIS. In winter, the signal is reversed and dH/dt is positive, however it is spatially less uniform (i.e., the areas with a reversed signal are more extensive) than the summer signal. The largest signals occur along the margins of the AIS, where temperature and accumulation rates are relatively high. A notable feature is the anomalous pattern along the Weddell Sea coast, i.e., the Antarctic Peninsula (AP) and Coats Land (78°S, 30°W). The driving force of this anomalous pattern is accumulation:

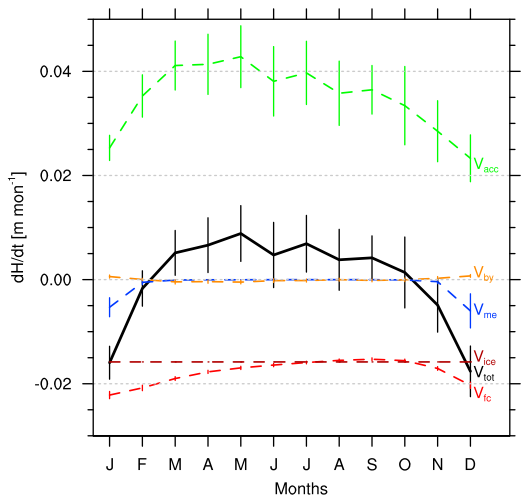

Figure 2. Monthly surface elevation changes (v_{tot}, black) and its components; accumulation (v_{acc}, green), firn compaction (v_{fc}, red), snowmelt (v_{me}, blue), vertical downward movement of ice (v_{ice}, brown) and buoyancy effects (v_{by}, orange) as simulated by the firn densification model.

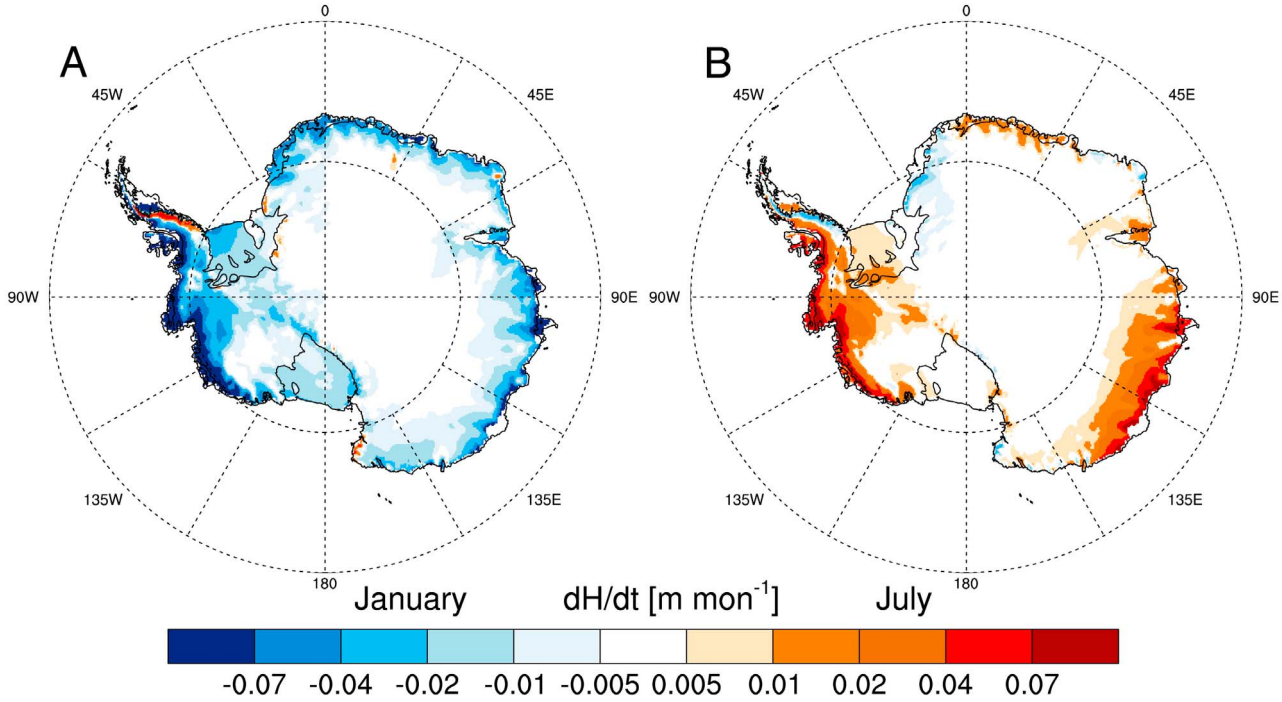

Figure 3. Spatial distribution of average monthly surface elevation changes (dH/dt) in (a) summer (January) and (b) winter (July).

for instance on the eastern AP, summer accumulation is three times higher than in winter, while on the western side it is the opposite. These accumulation characteristics are caused by the seasonally shifting direction of flow towards the mountain range of the AP.

[9] The amplitude of the seasonal elevation oscillation is defined as half the peak-to-peak value of a sine function fitted to the seasonal cycle in surface elevation. The average over all local amplitudes of the AIS is 0.026 m, but spatially there are large differences (Figure 4a). Amplitudes of less than 0.005 m are found on the interior East Antarctic plateau, an area with annual snowfall of 20–50 mm w.e. and very low T_s year round [*Lenaerts et al.*, 2012]. Along the margins of the AIS, higher temperatures and accumulation rates result in larger surface elevation oscillations (0.1–0.3 m). The largest amplitude (0.35 m) is simulated just inland of Getz ice shelf (75°S, 130°W) in West Antarctica. The FDM cannot be applied to ablation regions where sublimation and/or snowmelt exceed accumulation, i.e., where a firn layer cannot develop (white areas in Figure 4a).

[10] Figure 4b shows the phase of the elevation maximum, which generally occurs in late winter, spring or even early summer depending on the timing of the maximum in accumulation. Along the Weddell Sea coast, the anomalous pattern again emerges, with an elevation maximum in late summer.

[11] Summed over the AIS, the average seasonal amplitude translates to a seasonal volume change of 340 km^3. If we account for the air-ice ratio in near-surface firn this equals the ~100 Gt average seasonal mass change as reported by *Lenaerts et al.* [2012], which corresponds to ~0.3 mm of global sea level equivalent and 4% of the total seasonal variation in ocean mass (6.8–8.5 mm) [*Chambers et al.*, 2004; *Willis et al.*, 2008].

[12] Few observations exist to verify the modeled seasonal oscillations. At Summit, Greenland, surface elevation oscillations of 0.125 m have been measured [*Zwally and Li*, 2002], which compares well with values found in Antarctic regions with similar climate conditions (~250 mm w.e. annual accumulation, $T_s \cong 244$ K and no snowmelt), such as coastal West-Antarctica.

[13] Time series of volume changes derived from ENVISAT RA over its region of coverage (red line in Figure 1; see Figure 4 for region of coverage) also show seasonal variations in surface elevation over the AIS. The seasonal amplitude from RA is considerably larger than the respective amplitude from the FDM. The spatial distribution of the amplitude of RA and the FDM qualitatively agree (Figures 4a–4c, note the different scale), with the lowest values in the East Antarctic interior and higher values along the margins. The average of the local seasonal amplitudes from the FDM, taken over the overlapping area, (0.029 m) represents 31% of the RA amplitude (0.093 m). While the seasonal variations in the RA time series are significantly larger than those simulated by the FDM, the phase is similar. The phase maximum in both methods occurs in the same season, although the RA surface elevation maximum is reached in late winter for most locations, which is on average 1–2 months earlier than in the FDM (Figures 4b, 4d, and 1). Interannual variations in both methods also show some similarities with a peak in surface elevation around 2006 and lowering thereafter (dots in Figure 1).

4. Discussion

[14] When comparing results of the FDM and RA on the seasonal time scale, we consider their differences as an upper bound on errors of either approach. In fact, there is no evident alternative method to assess RA or FDM seasonal

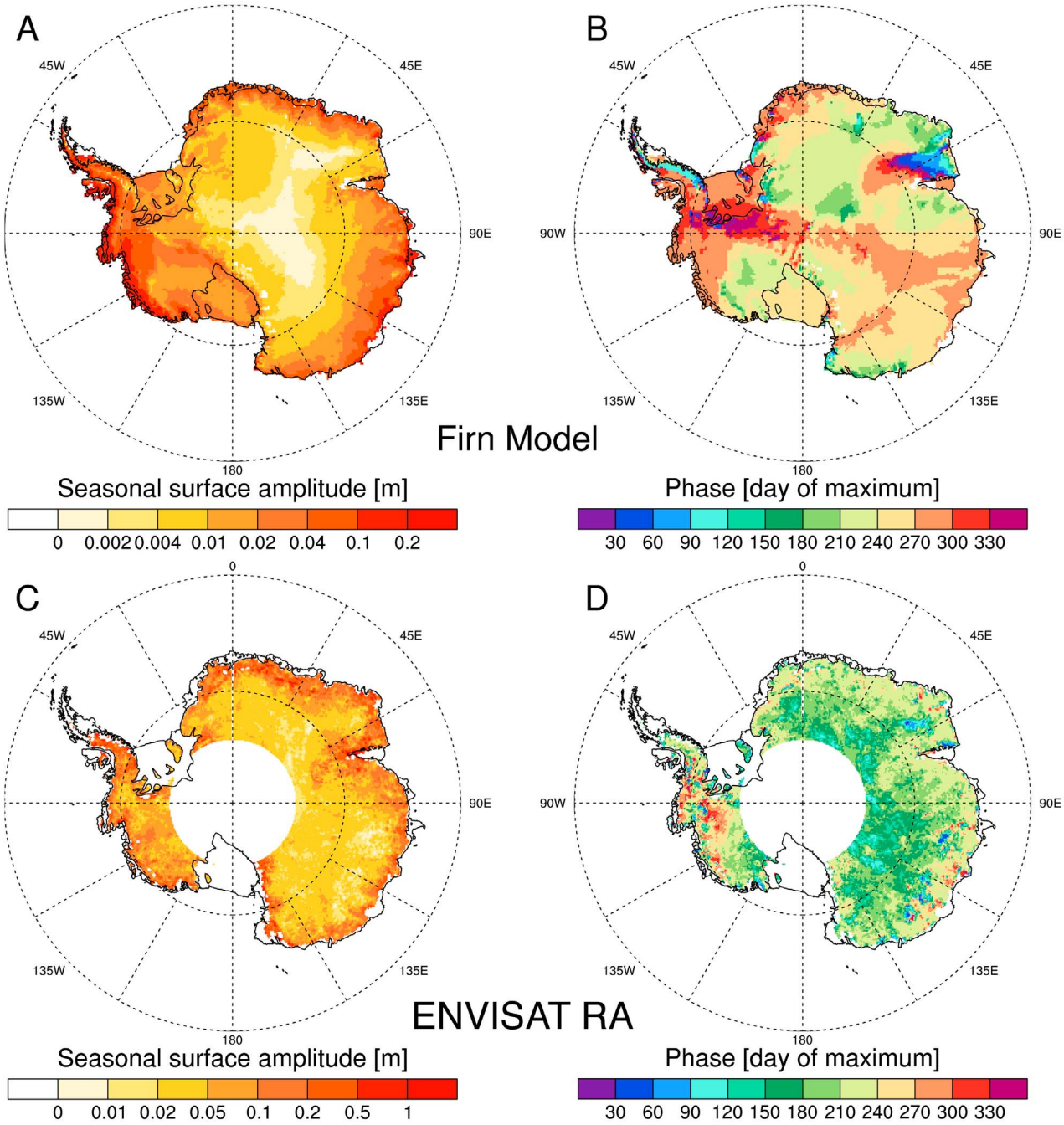

Figure 4. (a and c) Average amplitude (note the different scale) and (b and d) timing of phase maximum of the seasonal surface elevation oscillation, from the firn densification model (1979–2011; Figures 4a and 4b) and observed by ENVISAT radar altimetry (2002–2010; Figures 4c and 4d). In Figures 4a and 4b, white areas indicate locations were no firn layer is simulated, i.e., regions where annual snowmelt and/or sublimation are larger than accumulation. In Figures 4c and 4d, white areas indicate regions where no observations are available (e.g., the polar gap south of 81.5°S and regions with steep terrain), or where observations are excluded from the analysis (e.g., ice shelves).

errors on a regional or ice sheet scale, and no prior quantification of those errors. However, it is likely that most of the RA-FDM differences can be assigned to remaining systematic RA errors. An exaggeration of RA amplitudes is obvious in regions where RA amplitudes are on the order of, or larger than, the amount of annual snow accumulation. This is the case, for example, in Victoria Land (west of the Ross Ice Shelf) and around Lambert Glacier (74°S, 65°E) where RA amplitudes (Figure 4c) are significantly larger than the RACMO2 simulated accumulation [*Lenaerts et al.*, 2012].

[15] One crucial error source are time-variable relative contributions of surface and volume echos affecting the re-tracked heights [*Legrésy and Rémy*, 1998; *Arthern et al.*, 2001]. As mentioned in Section 2, here, we use the linear relation between the radar echo shape parameters and the re-tracked height, proposed by *Legrésy et al.* [2006], to build

an empirical height correction at each point on the ice sheet. *Lacroix et al.* [2009] showed the effectiveness of this correction for variations following strong wind events. A limitation of the empirical time-variable echo shape correction lies in the assumption of just a single relation existing between the echo shape parameters and the height correction, while there may be various modes of echo shape changes depending on i) the underlying physical process (wind, snow accumulation, densification) and ii) the time scale. The seasonal compaction implies that changes in the density of snow layers impact their dielectric response to radar waves. It is therefore possible that part of the seasonal echo shape change is not well represented in the empirical correction. These seasonal radar penetration effects may amount to up to several centimeters in amplitude and are therefore the first candidate to explain the RA contribution to the RA-FDM differences. Future studies may involve using the FDM to infer a density profile, to model the dielectric variations of the medium (alike *Lacroix et al.* [2008]) and to relate it to the RA variations.

[16] Orbital and reference frame issues [*Yi et al.*, 1997; *Dong et al.*, 2003] might also contribute to systematic seasonal effects in the RA measurements. They would show large-scale patterns independent of ice sheet geography, so an upper bound for such effects is given by the 2 cm level found in the Antarctic interior (Figure 4c).

[17] Some differences between the two datasets also arise from variations in ice flow observed by RA but not included in the FDM, where v_{ice} is assumed constant in time. Seasonal variations in ice flow may amount to the order of 10–20% in Greenland [e.g., *Zwally et al.*, 2002; *Joughin et al.*, 2008; *Rosenau et al.*, 2012]. In Antarctica, however, such variations are rare due to the limited supply of meltwater that could induce them [*Scambos et al.*, 2004]. Concerning flow variations on the interannual to decadal scale, *Rignot et al.* [2011] report a 9 Gt yr^{-1} annual change of Antarctic discharge (corresponding to 8 km^3 yr^{-1} of volume discharge). This is a minor contribution to the interannual variations of 50–500 km^3 that can be deduced from Figure 1.

5. Summary and Conclusions

[18] Using a combination of a firn densification model and a regional atmospheric climate model, we quantify the component of the seasonal volume change, or 'breathing', of the AIS, forced by the seasonal cycle in accumulation and temperature. High temperatures and low accumulation cause the surface to lower rapidly in austral summer, while in autumn, winter and spring the surface steadily rises, mainly due to higher accumulation rates. During the 32-year period under consideration (1979–2011), a clear annual cycle in surface elevation is found with an amplitude of 0.026 m averaged over the AIS, equivalent to a 340 km^3 volume oscillation. Across the ice sheet, amplitude values range from <0.002 m (high East Antarctic plateau) to >0.3 m in the coastal regions of West Antarctica. The phase of the seasonal cycle, with surface rising in winter and lowering in summer, is spatially consistent across the AIS, except for the Weddell Sea coast; here the phase of the seasonal cycle in accumulation and hence surface elevation is reversed. The modeled seasonal variations in surface elevation explain ~31% of the seasonal signal in ENVISAT radar altimetry data with a phase that is similar (maximum in late winter or early spring). These results can be used to correct surface elevation changes derived from altimetric records over short time intervals or with sparse temporal sampling.

[19] **Acknowledgments.** We thank Ben Smith and one anonymous reviewer for their valuable comments. This work was supported by the Netherlands Polar Program of NWO/ALW and the ice2sea project, funded by the European Commission's 7th Framework Programme through grant 226375, ice2sea manuscript 111.

[20] The Editor thanks Ben Smith and one anonymous reviewer for their assistance in evaluating this paper.

References

Arthern, R. J., D. J. Wingham, and A. L. Ridout (2001), Controls on ERS altimeter measurements over ice sheets: Footprint-scale topography, backscatter fluctuations, and the dependence of microwave penetration depth on satellite orientation, *J. Geophys. Res.*, *106*(D24), *33*, 471–484, doi:10.1029/2001JD000498.

Braithwaite, R. J., M. Laternser, and W. T. Pfeffer (1994), Variations of near-surface firn density in the lower accumulation area of the Greenland ice sheet, Pakitsoq, West Greenland, *J. Glaciol.*, *40*(136), 477–485.

Chambers, D. P., J. Wahr, and R. S. Nerem (2004), Preliminary observations of global ocean mass variations with GRACE, *Geophys. Res. Lett.*, *31*, L13310, doi:10.1029/2004GL020461.

Davis, C. H., Y. Li, J. R. McConnell, M. M. Frey, and E. Hanna (2005), Snowfall-driven growth in East Antarctic ice sheet mitigates recent sea-level rise, *Science*, *308*, 1898–1901, doi:10.1126/science.1110662.

Dong, D., T. Yunck, and M. Heflin (2003), Origin of the International Terrestrial Reference Frame, *J. Geophys. Res.*, *108*(B4), 2200, doi:10.1029/2002JB002035.

Gunter, B., T. Urban, R. Riva, M. Helsen, R. Harpold, S. Poole, P. Nagel, B. Schutz, and B. Tapley (2009), A comparison of coincident GRACE and ICESat data over Antarctica, *J. Geod.*, *83*, 1051–1060, doi:10.1007/s00190-009-0323-4.

Helsen, M., M. R. van den Broeke, R. S. W. van de Wal, W. J. van de Berg, E. van Meijgaard, C. H. Davis, Y. Li, and I. Goodwin (2008), Elevation changes in Antarctica mainly determined by accumulation variability, *Science*, *320*, 1626–1628, doi:10.1126/science.1153894.

Horwath, M., B. Legresy, F. Remy, F. Blarel, and J.-M. Lemoine (2012), Consistent patterns of Antarctic ice sheet interannual variations from ENVISAT radar altimetry and GRACE satellite gravimetry, *Geophys. J. Int.*, *189*, 863–876, doi:10.1111/j.1365-246X.2012.05401.

Intergovernmental Panel on Climate Change (2007), *Climate Change 2007: The Physical Science Basis. Contribution of Working Group I to the Fourth Assessment Report of the Intergovernmental Panel on Climate Change*, edited by S. Solomon et al., 996 pp., Cambridge Univ. Press, Cambridge, U. K.

Joughin, I., S. B. Das, M. A. King, B. E. Smith, I. M. Howat, and T. Moon (2008), Seasonal speedup along the western flank of the Greenland ice sheet, *Science*, *320*(5877), 781–783, doi:10.1126/science.1153288.

Lacroix, P., M. Dechambre, B. Legresy, F. Blarel, and F. Remy (2008), On the use of the dual-frequency ENVISAT altimeter to determine snowpack properties of the Antarctic ice sheet, *Remote Sens. Environ.*, *112*(4), 1712–1729, doi:10.1016/j.rse.2007.08.022.

Lacroix, P., B. Legrésy, F. Rémy, F. Blarel, G. Picard, and L. Brucker (2009), Rapid change of the snow surface properties at Vostok, East Antarctica, revealed by altimetry, *Remote Sens. Environ.*, *113*, 2633–2641, doi:10.1016/j.rse.2009.07.019.

Lee, H., C. K. Shum, I. M. Howat, A. Monaghan, Y. Ahn, J. Duan, J.-Y. Guo, C.-Y. Kuo, and L. Wang (2012), Continuously accelerating ice loss over Amundsen Sea catchment, West Antarctica, revealed by integrating altimetry and GRACE data, *Earth Planet. Sci. Lett.*, *321–322*, 74–80, doi:10.1016/j.epsl.2011.12.040.

Legrésy, B., and F. Rémy (1998), Using the temporal variability of satellite radar altimetry observations to map surface properties of the Antarctic ice sheet, *J. Glaciol.*, *44*(147), 197–206.

Legrésy, B., F. Rémy, and F. Blarel (2006), Along track repeat altimetry for ice sheets and continental surface studies, in *Proceedings of Symposium on 15 Years of Progress in Radar Altimetry, Venice, Italy, 13–18 March 2006*, *Eur. Space Agency Spec. Publ.*, *ESA SP-614*, 181.

Lenaerts, J. T. M. and M. R. van den Broeke (2012), Modeling drifting snow in Antarctica with a regional climate model: 2. Results, *J. Geophys. Res.*, *117*, D05109, doi:10.1029/2010JD015419.

Lenaerts, J. T. M., M. R. van den Broeke, W. J. van de Berg, E. van Meijgaard, and P. Kuipers Munneke (2012), A new, high-resolution surface mass balance map of Antarctica (1979–2010) based on regional atmospheric climate modeling, *Geophys. Res. Lett.*, *39*, L04501, doi:10.1029/2011GL050713.

Ligtenberg, S. R. M., M. M. Helsen, and M. R. van den Broeke (2011), An improved semi-empirical model for the densification of Antarctic firn, *Cryosphere*, *5*, 809–819, doi:10.5194/tc-5-809-2011.

Lythe, M. B., D. G. Vaughan, and the BEDMAP Consortium (2001), BEDMAP: A new ice thickness and subglacial topographic model of Antarctica, *J. Geophys. Res.*, *106*(B6), 11,335–11,351, doi:10.1029/2000JB900449.

Pritchard, H. D., S. R. M. Ligtenberg, H. A. Fricker, D. G. Vaughan, M. R. van den Broeke, and L. Padman (2012), Antarctic ice-sheet loss driven by basal melting of ice shelves, *Nature*, *484*, 502–505, doi:10.1038/nature10968.

Rignot, E., I. Velicogna, M. R. van den Broeke, A. Monaghan, and J. Lenaerts (2011), Acceleration of the contribution of the Greenland and Antarctic ice sheets to sea level rise, *Geophys. Res. Lett.*, *38*, L05503, doi:10.1029/2011GL046583.

Rosenau, R., R. Dietrich, and M. Baessler (2012), Temporal flow variations of major outlet glaciers in Greenland using LANDSAT data, paper presented at IGARSS 2012: IEEE International Geoscience and Remote Sensing Symposium, Inst. of Electr. and Electron. Eng., Munich, Germany, 22–27 July.

Scambos, T. A., J. A. Bohlander, C. A. Shuman, and P. Skvarca (2004), Glacier acceleration and thinning after ice shelf collapse in the Larsen B embayment, Antarctica, *Geophys. Res. Lett.*, *31*, L18402, doi:10.1029/2004GL020670.

Thomas, R., C. Davis, E. Frederick, W. Krabill, Y. Li, S. Manizade, and C. Martin (2008), A comparison of Greenland ice-sheet volume changes derived from altimetry measurements, *J. Glaciol.*, *54*(185), 203–212, doi:10.3189/002214308784886225.

Van den Broeke, M. R., J. Bamber, J. Lenaerts, and E. Rignot (2011), Ice sheets and sea level: Thinking outside the box, *Surv. Geophys.*, *32*, 495–505, doi:10.1007/s10712-011-9137-z.

Velicogna, I. (2009), Increasing rates of ice mass loss from the Greenland and Antarctic ice sheets revealed by GRACE, *Geophys. Res. Lett.*, *36*, L19503, doi:10.1029/2009GL040222.

Willis, J. K., D. P. Chambers, and R. S. Nerem (2008), Assessing the globally averaged sea level budget on seasonal to interannual timescales, *J. Geophys. Res.*, *113*, C06015, doi:10.1029/2007JC004517.

Yi, D., C. R. Bentley, and M. D. Stenoien (1997), Seasonal variation in the apparent height of the East Antarctic ice sheet, *Ann. Glaciol.*, *24*, 191–198.

Zwally, H. J., and J. Li (2002), Seasonal and interannual variations of firn densification and ice-sheet surface elevation at the Greenland Summit, *J. Glaciol.*, *48*(161), 199–207.

Zwally, H. J., W. Abdalati, T. Herring, K. Larson, J. Saba, and K. Steffen (2002), Surface melt-induced acceleration of Greenland ice-sheet flow, *Science*, *297*(5579), 218–222, doi:10.1126/science.1072708.